ACS Photonics

Letter

pubs.acs.org/journal/apchd5

Excitonic Optical Tamm States: A Step toward a Full Molecular–Dielectric Photonic Integration

Sara Núñez-Sánchez,*[,†,‡] Martin Lopez-Garcia,[‡] Mohamed M. Murshidy,[§,∥,⊥] Asmaa Gamal Abdel-Hady,[⊥] Mohamed Serry,[⊥] Ali M. Adawi,[§] John G. Rarity,[‡] Ruth Oulton,[‡,#] and William L. Barnes[†]

[†]School of Physics and Astronomy, University of Exeter, Exeter EX4 4QL U.K.

[‡]Photonics Group, Department of Electrical and Electronic Engineering, University of Bristol, Bristol BS8 1TH U.K.

[§]Department of Physics and Mathematics, University of Hull, Kingston upon Hull HU6 7RX U.K.

[∥]Department of Physics, Faculty of Science, Helwan University, Helwan, 11792 Egypt

[⊥]Department of Mechanical Engineering, The American University in Cairo, Cairo 11835 Egypt

[#]School of Physics, University of Bristol, Bristol BS8 1TL U.K.

Supporting Information

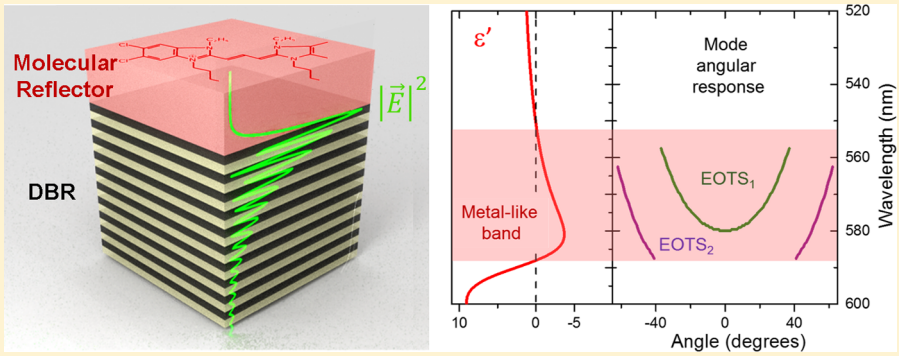

ABSTRACT: We report the first experimental observation of an excitonic optical Tamm state supported at the interface between a periodic multilayer dielectric structure and an organic dye-doped polymer layer. The existence of such states is enabled by the metal-like optical properties of the excitonic layer based on aggregated dye molecules. Experimentally determined dispersion curves, together with simulated data, including field profiles, allow us to identify the nature of these new modes. Our results demonstrate the potential of organic excitonic materials as a powerful means to control light at the nanoscale, offering the prospect of a new alternative photonic building block for nanophotonics designs based on molecular materials.

KEYWORDS: *exciton, surface modes, Tamm states, J-aggregates, thin films, organic, molecular materials, plasmons*

Light confinement at nanoscale dimensions is now a routine matter and is primarily achieved in the visible and near-infrared part of the electromagnetic spectrum by making use of the plasmon modes associated with metallic nanostructures.[1] The key advantages that resonant plasmon modes bring are enhanced electromagnetic field strengths and subwavelength field confinement with, for example, a number of strong potential applications in areas such as quantum technology.[2] A number of alternatives to metals have now been explored,[3−5] including graphene[6] and other atomically thin materials.[7] Very recently interest has been rekindled in using molecular resonances, especially in the form of molecular excitonic states.[8,9] Such materials may exhibit a strong enough resonant excitonic response that the real part of the associated permittivity becomes negative in the vicinity of the resonance. When this happens the excitonic material may take on a reflective, metallic appearance.[10,11] Early work in this area involved molecular crystals, for which a negative real permittivity was achieved at low temperatures.[12] In the 1970s Philpott and co-workers showed that organic excitonic crystals may support surface exciton-polaritons,[12,13] analogous to the surface plasmon-polaritons supported by metals.[14] Recently surface exciton-polaritons supported by dye-doped polymers have been experimentally demonstrated,[8,9] and localized (particle-like) exciton-polaritons theoretically predicted.[8,15,16] Here we provide the first demonstration that molecular materials can also be used as building blocks to create another class of nanophotonic mode, specifically optical Tamm states (OTSs). By extending the range of nanophotonic modes supported by molecular materials, our results open the exciting prospect of using molecular materials to replace metals as a

Received: January 25, 2016
Published: April 13, 2016

DOI: 10.1021/acsphotonics.6b00060
ACS Photonics 2016, 3, 743−748

means to control light at the nanoscale in an integrated fully dielectric scheme.[17]

OTSs are optical modes that occur at the interface between two reflective photonic structures,[18] with fields that decay with distance from the interface that supports them. Demonstration of the existence of these modes has previously been performed using two periodic dielectric stacks,[18] or a combination of a periodic dielectric stack and a metallic reflector.[19] When the reflector is a metal thin film, the modes are named Tamm plasmons, which have shown potential applications as sensors,[20] as lasers with enhanced directional emission,[21,22] and for control of spontaneous optical emission of single-photon emitters.[23] Control of polarization and angular response has been obtained by using pattern processing to impose nanostructure on the metallic reflector layer[22,24] in order to laterally confine the modes.[23] Here we show that OTSs with a tailored dispersion curve can also occur between a periodic dielectric stack and an organic (molecular) reflector thin film, giving a new class of OTS mode, an excitonic optical Tamm state (EOTS). The limited wavelength range over which metal-like reflectance occurs for the excitonic layer defines a truncated dispersion of the EOTS modes without the need for patterning of the excitonic layer.

In this Letter we demonstrate the existence of EOTS modes between a truncated 1-D photonic crystal (distributed Bragg reflector, DBR) and a polymer layer heavily doped by J-aggregate molecules (the excitonic layer). Light may excite an EOTS when illumination takes place at an incident angle that allows momentum matching to the EOTS to be achieved. The spectrally narrow range over which the metal-like behavior occurs limits the spectral range over which EOTS may be supported. Below we demonstrate that one can tailor the EOTS dispersion curve and its cutoff wavelengths through the overlap of the momentum-matching mode condition and the limited wavelength range of metal-like properties of the excitonic layer. In what follows, we first describe the characteristic dispersion curves associated with the EOTS based on the optical properties of our excitonic material and on the DBR stopband position. We then present an experimental observation of EOTS excitation in three photonic structures, each showing a different mode cutoff wavelength.

The propagation condition for an OTS in a multilayer structure DBR/(thin film) requires that the thin film show a high reflectivity response within the stopband of the DBR stack.[19] Metals such as silver can fulfill this condition over the entire visible wavelength range. A dielectric medium doped with an excitonic species exhibiting a strong absorption resonance may be modeled using the classical single Lorentz oscillator model:

$$\epsilon_r(\omega) = 1 + \chi(\omega) + \frac{f_0 {\omega_0}^2}{{\omega_0}^2 - \omega^2 + i\gamma_0\omega}$$

where the resonance frequency (ω_0) corresponds to the exciton transition, γ_0 is the damping rate, and f_0 is the reduced oscillator strength; the term χ takes into account the background susceptibility, while the reduced oscillator strength is proportional to the concentration of excitonic species. If the oscillator strength is strong enough, then the real part of the permittivity will take negative values over a limited wavelength range, giving a colored metallic luster to the organic layer.[10,11] In this work we take the values for the resonance frequency, the damping parameter, and background susceptibility from previous work.[8] For our theoretical study we first considered an excitonic layer with a value of the reduced oscillator strength around unity. Using this oscillator strength, the real part of the permittivity attains negative values over a wavelength band of 100 nm centered on the short-wavelength side of the excitonic transition (from 490 nm to just below 590 nm). The excitonic layer fulfills the condition of high reflectance only in this wavelength range (see Supporting Information, section 1). For the DBR structure we considered a stack formed of nine pairs of silicon oxide and silicon nitride layers deposited on top of a glass substrate, similar to our experimental samples, but with a central wavelength of 490 nm. The stopband edge of this DBR at normal incidence lies within the high-reflectance wavelength band of the excitonic layer. All simulations and experimental results have been obtained with light incident from the substrate side.

Figure 1a shows the simulated reflectance at normal incidence of the DBR stack and two photonic structures

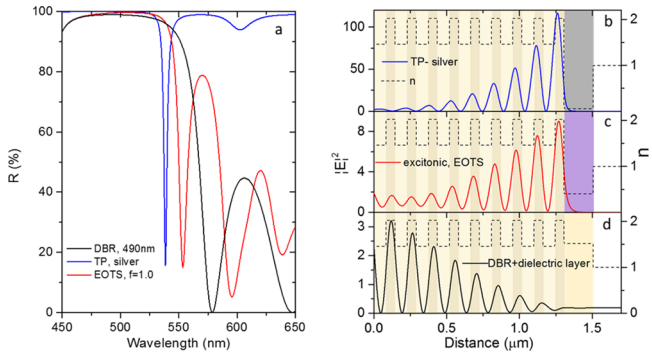

Figure 1. (a) Simulated reflection at normal incidence of a single DBR stack (λ_C = 490 nm, black line), an EOTS structure (red line) with an excitonic thin film with an oscillator strength value of 1, and a TP structure (blue line) with silver as metal top layer. Electric field intensity profile in the three structures at normal incidence for (b) TP mode (λ = 538 nm, blue line), (c) EOTS mode (λ = 553 nm, red line), and (d) stopband region (λ = 553 nm, black line). Black dotted lines represent the real part of the refractive index profile. Different color regions represent the layers with different optical properties. DBR is represented by cream (SiO_2, n = 1.46; first layer starting from substrate) and light brown (SiN_3, n = 2.02; first layer starting from reflector layer). Top layer is shown as gray for silver reflector (n = 0.06), lilac for the molecular reflector (n = 0.40), and light orange for nondoped PVA (n = 1.52, f = 0). White color represents air (n = 1).

supporting OTS, a DBR/(excitonic layer) that supports an EOTS mode and a DBR/(silver layer) that supports a Tamm plasmon mode (TP). Both reflector layers (excitonic layer and silver layer) have a thickness of 200 nm. The DBR shows a high reflectance close to 100% in the stopband range. However, in the two OTS structures we observe a sharp dip in the reflectance when the condition of mode excitation is fulfilled. Because the last DBR layer in contact with the reflector layer corresponds to the high refractive index quarter-wavelength layer (SiN_3), the mode condition will appear close to the low-energy band-edge of the DBR. If we compare the response of the TP structure with the EOTS structure, we observe that in the case of the TP structure the reflectance is close to unity over the whole wavelength range except when the mode is excited. This high reflectance is due to the mirror properties of the silver layer over all of the wavelength range examined. However, in structures supporting EOTSs, reflectance follows

DOI: 10.1021/acsphotonics.6b00060
ACS Photonics 2016, 3, 743−748

the individual DBR response outside the metal-like range of the excitonic material, showing a sharp dip only when the mode condition is achieved. This is because the high-reflectance band of the excitonic layer occurs only over a limited wavelength range; outside this wavelength range the excitonic layer behaves as a simple dielectric without significantly affecting the DBR response, although the presence of this dielectric layer shifts the Fabry–Perot oscillations associated with the DBR to longer wavelengths when compared to the response of the DBR alone.

To confirm the nature of the EOTS mode, we need to examine the field intensity profile characteristic of an OTS. Figure 1b shows the field intensity profile obtained for the TP mode; it is seen to oscillate and to decay with distance away from the interface between the metal and the DBR stack. The decay profile within the DBR is modulated by the periodic variation of the refractive index of the DBR, while it decays smoothly into the metal medium. Comparing Figure 1b and c, the electric field profile obtained for the EOTS shows the same features as the TP, confirming that the EOTS has a field confinement that is similar to the TP. In order to confirm that the field profile is due only to the presence of excitonic species embedded in the polymer, we have calculated the field profile at the same illumination conditions (wavelength and angle) for a DBR stack covered by an organic thin film layer but with a null oscillator strength. The field intensity profile that we obtain is an oscillatory field that increases with distance away from the interface between the dielectric film and the DBR stack (see Figure 1d), as is expected when an interference effect is responsible for the high reflectance in the stopband of the DBR stack.[25]

Due to the similarities of the TP and EOTS, the dispersion curves of these modes have some properties in common. With our DBR structures a TP will be located close to the low-energy band-edge.[19] We can thus use this low-energy stopband-edge as a reference to estimate the dispersion curves. We have used two different methods to obtain the dispersion curves of the EOTS, following the position of the dip in the reflectance below the low-energy band-edge and by matching the mode condition equation (see details in Supporting Information, section 2). Note that the stopband-edge positions of a DBR stack depend strongly on the polarization and in-plane component of the wavevector. We thus expect that the mode condition should follow a similar trend to that of the DBR stopband edges. In the case of a TP structure, the mode condition can be met across all of the visible wavelength range; however, the EOTS excitation is necessarily limited to the region where the excitonic layer has permittivity values sufficiently negative to obtain a metal-like reflectance. Consequently the TP shows a continuous dispersion curve, while the dispersion curves of the EOTS are truncated. These results show that it may be possible to design EOTS modes that can be excited only at normal incidence (zero in-plane component of the wavevector) or for a finite range of in-plane components of the wavevector corresponding to oblique propagation. The truncation (cutoff) wavelengths are delimited by the convolution of the low-energy stopband-edge of the DBR and the metal-like reflectance band of the excitonic layer.

Figure 2 shows the dispersion curves obtained for TP and EOTS in structures formed by two different DBR stacks (of central wavelengths 490 and 590 nm) with silver and a molecular (TDBC) reflector of 200 nm thickness. While the TP modes are allowed for all values of the in-plane component of the wavevector in the two different multilayer structures, the

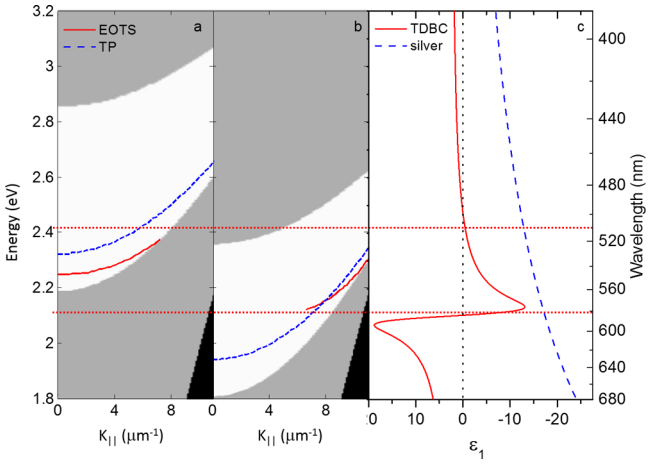

Figure 2. (a, b) DBR stopband representation for Pp-polarized light (TM) for two different DBRs with central wavelengths of 490 nm (a) and 590 nm (b). White areas represent the stopband region where the reflectance is higher than 70%. The black regions correspond to areas below the light line that are not directly accessible by incident light. The gray areas represent all the regions outside the stopband where the reflectance is lower than 70%. Continuous red lines represent the dispersion curves for the EOTS modes supported by the DBR topped with a layer of 200 nm of excitonic material ($f_0 = 1$). Blue dashed lines represent the TP dispersion for the same DBR topped by 200 nm of silver. (c) Values of the real part of the permittivity for a dielectric medium with a strong resonance at 590 nm and an oscillator strength of 1 and for silver from ref 31. Red dotted lines mark the spectral region where the real part of the permittivity of the excitonic layer reaches negative values of the permittivity.

EOTS can be excited only over restricted illumination conditions. In the structure with a DBR with a central wavelength around 490 nm we can excite modes only near normal incidence ($k_{||} = 0$), while for the structure with a DBR central wavelength of 590 nm the EOTS mode can be excited only by light impinging close to grazing incidence (large $k_{||}$ values). Therefore, by simply controlling the position of the DBR low-energy stopband-edge relative to the optical properties of the excitonic medium, it is possible to obtain an optical device with a controlled directional response without the need for surface nanostructure.

Three different multilayer structures supporting EOTS were fabricated using different DBR structures but with the same excitonic layer. The DBR mirrors were fabricated using nine pairs of silicon dioxide and silicon nitride layers deposited by plasma-enhanced chemical vapor deposition on top of a glass substrate. The mirrors were designed with central wavelengths (λ_C) lying in the range 500 to 585 nm (DBR-500, DBR-520, DBR-585). The highly reflective excitonic layers were spin-cast on top of the DBR mirrors from solutions of the molecular dye TDBC and poly(vinyl alcohol) (PVA) in water. Here we used TDBC molecules as excitonic species (5,6-dichloro-2-[[5,6-dichloro-1-ethyl-3-(4-sulfobutyl)benzimidazol-2-ylidene]-propenyl]-1-ethyl-3-(sulfobutyl)benzimidazolium hydroxide, sodium salt, inner salt), with an associated excitonic resonance centered at a wavelength of 590 nm. In appropriate solutions these molecules form J-aggregates; the excitons delocalize in such aggregates leading to (i) a stronger effective dipole moment associated with the exciton and (ii) a narrower excitonic resonance (arising from exchange narrowing).[26] This strong dipole moment makes these systems well suited to our purpose since this helps produce an optical response that is

DOI: 10.1021/acsphotonics.6b00060
ACS Photonics 2016, 3, 743–748

strong enough to exhibit a negative permittivity. The TDBC−PVA solutions were prepared by mixing a PVA−water solution with a TDBC−water solution as explained elsewhere.[8] All TDBC/PVA spun films deposited were designed to yield a 200 nm thickness for the excitonic layer. The optical properties and oscillator parameters of the TDBC/PVA layer were determined in a previous work through reflection and transmission spectroscopy of TDBC/PVA films spun on glass at normal incidence.[8]

Angle- and polarization-resolved reflection maps of the compound structures were obtained using Fourier imaging spectroscopy.[27] The samples were illuminated from the substrate side by projecting the output of a fiber coupled to a white light source (Thorlabs OS-L1) through a high numerical aperture objective lens, Zeiss 63X Plan-Neofluar (NA = 0.75, WD = 1.2 mm). The reflected pattern generated at the back focal plane of the objective was then scanned with a fiber coupled to a spectrometer (Ocean200+) so as to obtain the angle- and polarization-resolved reflectance of the structure for all angles within the NA of the objective lens (θ_{max} = 48° in our case). Angles were then translated into in-plane components of the incident wavevector (k_{II}) for comparison with the calculated dispersion curves.

Figure 3 shows the experimental reflectance maps for s-polarized light as a function of energy and in-plane wavevector

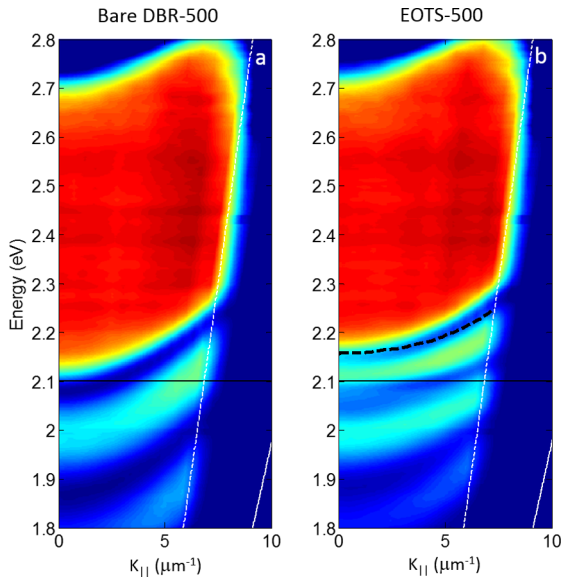

Figure 3. Experimental s-polarized (TE) reflectance maps for (a) a bare DBR structure composed of a DBR with a central wavelength of 500 nm (DBR-500) and (b) an EOTS structure composed of an excitonic layer of 200 nm on top of a DBR with a central wavelength of 500 (EOTS-500). Black dashed line corresponds to the calculated dispersion curves for the EOTS TE modes. Black continuous lines indicate the exciton absorption resonance of the J-aggregate molecules at 2.1 eV. White dashed lines represent the numerical aperture of the objective used in the reflectance collection and illumination. The continuous white lines correspond to the light cone.

for a DBR multilayer (bare DBR-500) and an EOTS structure formed by the same DBR but with a 200 nm excitonic layer on top (EOTS-500). The DBR-500 shows a high-reflectance stop-band (colored in red) equivalent to the white areas presented in Figure 2a,b. When the excitonic layer is deposited on top of the DBR, we observe a change in the reflectance response of the EOTS-500 in comparison with the DRB-500 structure. The excitation of the EOTS mode leads to a strong dip in reflectance located below yet close to the low-energy band-edge of the DBR. The high-reflectance band of the excitonic layer occurs only over a limited wavelength range; therefore outside this wavelength range the EOTS-500 structure should have a similar optical response to the DBR-500. It can be clearly observed in Figure 3 below 2.1 eV and above 2.3 eV. Due to this specific characteristic of EOTS modes, it is not possible to determine only from experimental data when the EOTS mode condition ends so that the dip observed in reflectance is then only related with the low-energy band-edge of the bottom DBR structure. Therefore, theoretical dispersion curves are plotted on top of the experimental results to visualize the cutoff wavelengths for the different combination of DBRs and the excitonic layer. We would like to note that cutoff wavelengths have been studied in detail, analyzing the optical field profiles associated with the dips observed in reflectance (see Supporting Information, section 3).

Figure 4 shows the experimental reflectance maps for s- and p-polarized light as a function of energy and in-plane

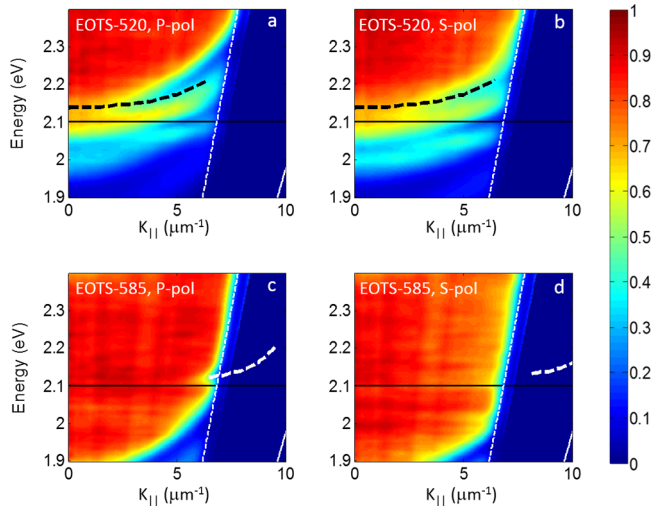

Figure 4. Experimental reflectance maps for an EOTS structure composed of a DBR with a central wavelength of 520 nm for (a) p-polarized light and (b) s-polarized light. Black dashed curved lines correspond to the calculated dispersion curves for the EOTS-520 modes. Black continuous lines indicate the exciton absorption resonance of the J-aggregate molecules at 2.1 eV. White dotted lines represent the numerical aperture of the objective used in the reflectance collection and illumination. The continuous white lines correspond to the light cone. Experimental reflectance maps for an EOTS structure composed of a DBR with a central wavelength of 585 nm for (c) p-polarized light and (d) s-polarized light. In this case the dispersion curves are plotted by thick white dashed lines.

wavevector for two new EOTS structures. The EOTS-520 and EOTS-585 multilayer structures are formed by a 200 nm excitonic layer deposited on top of DBRs with central wavelengths at 520 and 585 nm, respectively. EOTS are supported by all three structures (EOTS-500, EOTS-520, and EOTS-585). For the multilayer structure comprising a DBR with a central wavelength of 500 nm the EOTS TE mode may be excited for all angles accessible within our objective numerical aperture (Figure 3b). The absolute value of the dip in reflectance observed is similar for the entire measured wavevector range. When the central wavelength of the DBR is

DOI: 10.1021/acsphotonics.6b00060
ACS Photonics 2016, 3, 743−748

shifted to lower energies (EOTS-520), the dispersion curve is flattened and red-shifted (Figure 4a,b). In this case it is noticeable that the coupling efficiency is not uniform for all excitation conditions; in fact the mode is weak at normal incidence, while the coupling efficiency is stronger for larger in-plane wave vectors. This effect is due to a fast change of the optical properties of the polymer layer within the wavelength range of the excitonic resonance (see Figure 2c). Modal excitation at normal incidence (zero in-plane component) is achieved in both multilayer structures (EOTS-500, EOTS-520) and both polarizations. However, when the central band of the DBR is at lower energies close to the molecular resonance frequency (as for the EOTS-585 structure), the modes can be excited only by larger components of the in-plane wavevector (Figure 4c,d).

Optical Tamm states are characterized by a splitting between TE and TM polarized modes that increases quadratically as a function of the in-plane wavevector.[18] Therefore, in the case of EOTS, for the same photonic structure we should observe different cutoff wavelengths for TE and TM modes (detailed in Supporting Information, section 4). For comparison purposes Figure 5 shows the s-polarized (TE) and p-polarized (TM) experimental reflectance response for EOTS-520 and EOTS-585 samples at different angles (in-plane wavevectors). At normal incidence (zero in-plane wavevector), EOTS-520 shows the same reflectance response for both polarizations, having the same excitation condition for TM and TE modes. Because the low-energy band-edge is very close to the excitonic resonance (at 2.1 eV), the dip in reflectance does not recover completely, thus diminishing the quality factor of the mode. However, for large in-plane wavevectors under illumination at the same incident angle, the energy that matches the mode condition will be lower for the TE mode than for the TM mode (see Figure 5b). This is due to the fact that at large angles the low-energy band-edge of the DBR is shifted to higher energies for a p-polarized light than for an s-polarized light, while the high-reflectance wavelength band of the excitonic layer remains fixed. Interestingly, the designed structures show a clear splitting between TE and TM modes, which in some cases might result in a TE- or TM-only propagation for a particular in-plane wavevector. This was seen for the EOTS-585 structure, where only a TM mode is observed in our measurement range (see Figure 4c,d). At normal incidence (zero in-plane wavevector), EOTS-585 shows the same reflectance response for both polarizations, without observing any dip in reflectance (no TE or TM mode excitation in Figure 5c). This is because the low-energy band-edge of the DBR of the EOTS-585 structure at normal incidence is located away from the energy range where the high-reflectance band of the excitonic resonance is located. However, for large in-plane wavevectors, we are able to observe a dip in reflectance for p-polarized light, while the s-polarized light response remains very similar to that of a bare DBR (see Figure 5d). As for EOTS-520 structures this is due to the fact than the DBR low-energy band-edge is shifted to higher energies for the p-polarized light than for s-polarized light. These results show that it is possible to obtain OTS modes by design with restrictions on polarization and angular directionality by selecting the optical properties of the excitonic materials employed.

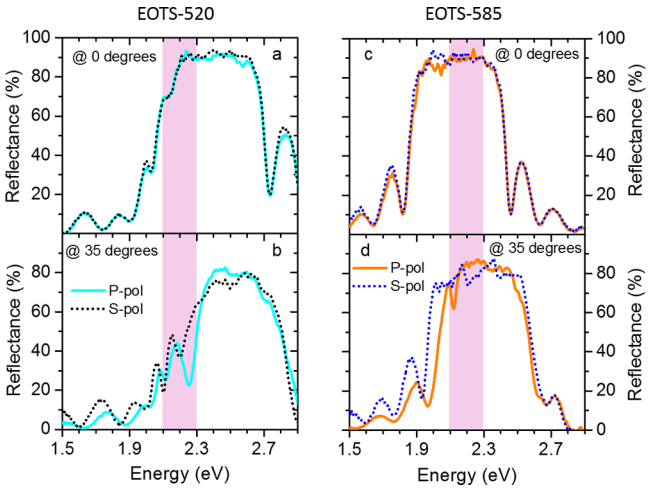

Figure 5. Experimental s-polarized and p-polarized reflectance response of an EOTS structure composed of a DBR with a central wavelength of 520nm for incident angles of (a) 0 degrees and (b) 35 degrees. EOTS structure composed of a DBR with a central wavelength of 585 nm at incident angles of (c) 0 degrees and (d) 35 degrees. The pink areas indicate the wavelength range where the excitonic layer shows a metal-like reflectance.

In conclusion, we have reported the observation of excitonic optical Tamm states using an organic layer as a reflector layer, opening a new route to design tailored photonic modes by harnessing the metal-like properties of heavily dye-doped polymer materials to create all-dielectric nanophotonic structures. EOTS modes with different propagation and polarization conditions were obtained by matching metal-like restricted properties of molecular materials and mode conditions. Such an approach will allow the power of supramolecular chemistry to be harnessed in the design and fabrication of structures to manipulate light in new ways,[28] for example using DNA origami.[29] The relatively narrow spectral range of operation might be extended through the use of co-doped thin films containing multiple species.[11,30] Moreover, the use of excitonic materials in nanophotonics leads to a number of intriguing open questions. A potentially attractive benefit over metals is that the detailed properties of these materials may be controlled by optical (and possibly electrical) pumping, perhaps yielding active functionality. Such possibilities also lead us to suggest that these structures might allow other fascinating questions to be addressed, for example what happens to quantum emitters embedded in such materials and whether they might be harnessed for photonic quantum technologies.[2]

■ ASSOCIATED CONTENT

Supporting Information

The Supporting Information is available free of charge on the ACS Publications website at DOI: 10.1021/acsphotonics.6b00060. All data presented in this paper can be accessed free of charge from the Open Research Exeter (ORE) database at URI: hdl.handle.net/10871/21111.

Reflectance response of thin film molecular reflectors as a function of the reduced oscillator strength; detailed description of the methods used to obtain the dispersion curves of the excitonic optical Tamm states; analysis of the obtained wavelength cutoff values for both polarized modes (TE, TM) (PDF)

DOI: 10.1021/acsphotonics.6b00060
ACS Photonics 2016, 3, 743−748

AUTHOR INFORMATION

Corresponding Author

*E-mail: sara.nunez.sanchez@gmail.com.

Notes

The authors declare no competing financial interest.

ACKNOWLEDGMENTS

W.L.B. gratefully acknowledges the support of The Leverhulme Trust and the Engineering and Physical Sciences Research Council of U.K. (grant EP/K041150/1). M. S. would like to acknowledge the funding from The American University in Cairo (AUC) through a Faculty Support Research Grant.

REFERENCES

(1) Gramotnev, D. K.; Bozhevolnyi, S. I. Plasmonics beyond the Diffraction Limit. *Nat. Photonics* **2010**, *4*, 83−91.

(2) Tame, M. S.; McEnery, K. R.; Ozdemir, S. K.; Lee, J.; Maier, S. A.; Kim, M. S. Quantum Plasmonics. *Nat. Phys.* **2013**, *9*, 329−340.

(3) Kalusniak, S.; Sadofev, S.; Henneberger, F. ZnO as a Tunable Metal: New Types of Surface Plasmon Polaritons. *Phys. Rev. Lett.* **2014**, *112*, 137401.

(4) Naik, G. V.; Liu, J.; Kildishev, A. V.; Shalaev, V. M.; Boltasseva, A. Demonstration of Al:ZnO as a Plasmonic Component for near-Infrared Metamaterials. *Proc. Natl. Acad. Sci. U. S. A.* **2012**, *109*, 8834−8838.

(5) Knight, M. W.; Coenen, T.; Yang, Y.; Brenny, B. J. M.; Losurdo, M.; Brown, A. S.; Everitt, H. O.; Polman, A. Gallium Plasmonics: Deep Subwavelength Spectroscopic Imaging of Single and Interacting Gallium Nanoparticles. *ACS Nano* **2015**, *9*, 2049−2060.

(6) Koppens, F. H. L.; Chang, D. E.; García de Abajo, F. J. Graphene Plasmonics: A Platform for Strong Light-Matter Interactions. *Nano Lett.* **2011**, *11*, 3370−3377.

(7) Manjavacas, A.; de Abajo, F. J. G. Tunable Plasmons in Atomically Thin Gold Nanodisks. *Nat. Commun.* **2014**, *5*, 3548.

(8) Gentile, M. J.; Núñez-Sánchez, S.; Barnes, W. L. Optical Field-Enhancement and Subwavelength Field-Confinement Using Excitonic Nanostructures. *Nano Lett.* **2014**, *14*, 2339−2344.

(9) Gu, L.; Livenere, J.; Zhu, G.; Narimanov, E. E.; Noginov, M. a. Quest for Organic Plasmonics. *Appl. Phys. Lett.* **2013**, *103*, 021104.

(10) Anex, B. G.; Simpson, W. T. Metallic Reflection from Molecular Crystals. *Rev. Mod. Phys.* **1960**, *32*, 466−476.

(11) Puthumpally-Joseph, R.; Sukharev, M.; Atabek, O.; Charron, E. Dipole-Induced Electromagnetic Transparency. *Phys. Rev. Lett.* **2014**, *113*, 163603.

(12) Philpott, M. R.; Brillante, A.; Pockrand, I. R.; Swalen, J. D. A New Optical Phenomenon: Exciton Surface Polaritons at Room Temperature. *Mol. Cryst. Liq. Cryst.* **1979**, *50*, 139−162.

(13) Pockrand, I.; Brillante, A.; Philpott, M. R.; Swalen, J. D. Observation of Exciton Surface Polaritons at Room Temperature. *Opt. Commun.* **1978**, *27*, 91−94.

(14) Zayats, A. V.; Smolyaninov, I. I.; Maradudin, A. a. Nano-Optics of Surface Plasmon Polaritons. *Phys. Rep.* **2005**, *408*, 131−314.

(15) Gentile, M. J.; Horsley, S. A. R.; Barnes, W. L. Localized Exciton-Polariton Modes in Dye-Doped Nanospheres: A Quantum Approach. *J. Opt.* **2016**, *18*, 015001.

(16) Cacciola, A.; Triolo, C.; Di Stefano, O.; Genco, A.; Mazzeo, M.; Saija, R.; Patanè, S.; Savasta, S. Subdiffraction Light Concentration by J-Aggregate Nanostructures. *ACS Photonics* **2015**, *2*, 971−979.

(17) Saikin, S. K.; Eisfeld, A.; Valleau, S.; Aspuru-Guzik, A. Photonics Meets Excitonics: Natural and Artificial Molecular Aggregates. *Nanophotonics* **2013**, *2*, 21−38.

(18) Kavokin, A.; Shelykh, I.; Malpuech, G. Lossless Interface Modes at the Boundary between Two Periodic Dielectric Structures. *Phys. Rev. B: Condens. Matter Mater. Phys.* **2005**, *72*, 233102.

(19) Kaliteevski, M.; Iorsh, I.; Brand, S.; Abram, R.; Chamberlain, J.; Kavokin, A.; Shelykh, I. Tamm Plasmon-Polaritons: Possible Electromagnetic States at the Interface of a Metal and a Dielectric Bragg Mirror. *Phys. Rev. B: Condens. Matter Mater. Phys.* **2007**, *76*, 165415.

(20) Auguié, B.; Fuertes, M. C.; Angelomé, P. C.; Abdala, N. L.; Soler Illia, G. J. A. A.; Fainstein, A. Tamm Plasmon Resonance in Mesoporous Multilayers: Toward a Sensing Application. *ACS Photonics* **2014**, *1*, 775−780.

(21) Badugu, R.; Lakowicz, J. R. Tamm State-Coupled Emission: Effect of Probe Location and Emission Wavelength. *J. Phys. Chem. C* **2014**, *118*, 21558−21571.

(22) Symonds, C.; Lheureux, G.; Hugonin, J. P.; Greffet, J. J.; Laverdant, J.; Brucoli, G.; Lemaitre, A.; Senellart, P.; Bellessa, J. Confined Tamm Plasmon Lasers. *Nano Lett.* **2013**, *13*, 3179−3184.

(23) Gazzano, O.; de Vasconcellos, S. M.; Gauthron, K.; Symonds, C.; Bloch, J.; Voisin, P.; Bellessa, J.; Lemaître, A.; Senellart, P. Evidence for Confined Tamm Plasmon Modes under Metallic Microdisks and Application to the Control of Spontaneous Optical Emission. *Phys. Rev. Lett.* **2011**, *107*, 247402.

(24) Lheureux, G.; Azzini, S.; Symonds, C.; Senellart, P.; Lemaître, A.; Sauvan, C.; Hugonin, J.-P.; Greffet, J.-J.; Bellessa, J. Polarization-Controlled Confined Tamm Plasmon Lasers. *ACS Photonics* **2015**, *2*, 842−848.

(25) Yeh, P.; Yariv, A.; Hong, C.-S. Electromagnetic Propagation in Periodic Stratified Media. I. General Theory. *J. Opt. Soc. Am.* **1977**, *67*, 438.

(26) Knoester, J. Optical Properties of Molecular Aggregates. In *Proceedings of the International School of Physics "Enrico Fermi"*. Course CXLIX; Agranovich, V. M.; La Rocca, G. C., Eds.; IOS Press: Amsterdam, 2002; pp 149−186.

(27) López-García, M.; Galisteo-López, J. F.; Blanco, A.; Sánchez-Marcos, J.; López, C.; García-Martín, A. Enhancement and Directionality of Spontaneous Emission in Hybrid Self-Assembled Photonic-Plasmonic Crystals. *Small* **2010**, *6*, 1757−1761.

(28) Lehn, J.-M. Toward Complex Matter: Supramolecular Chemistry and Self-Organization. *Proc. Natl. Acad. Sci. U. S. A.* **2002**, *99*, 4763−4768.

(29) Wang, M.; Silva, G. L.; Armitage, B. A. DNA-Templated Formation of a Helical Cyanine Dye J-Aggregate. *J. Am. Chem. Soc.* **2000**, *122*, 9977−9986.

(30) Würthner, F.; Kaiser, T. E.; Saha-Möller, C. R. J-Aggregates: From Serendipitous Discovery to Supramolecular Engineering of Functional Dye Materials. *Angew. Chem., Int. Ed.* **2011**, *50*, 3376−3410.

(31) Johnson, P.; Christy, R. Optical Constants of the Noble Metals. *Phys. Rev. B* **1972**, *6*, 4370−4379.

DOI: 10.1021/acsphotonics.6b00060
ACS Photonics 2016, 3, 743−748